Water-Enhanced Catalysis of CO Oxidation on Free and Supported Gold Nanoclusters

Angelo Bongiorno and Uzi Landman
School of Physics, Georgia Institute of Technology, Atlanta, Georgia 30332-0430, USA
(Received 5 May 2005; published 1 September 2005)

The enhancement by water molecules of the catalytic activity of gas-phase and supported gold nanoclusters toward CO oxidation is investigated with first-principles calculations. Coadsorption of H_2O and O_2 leads to formation of a complex well bound to the gold cluster, even on a defect-free MgO(100) support. Formation of the complex involves partial proton sharing between the adsorbates, that in certain configurations results in proton transfer leading to the appearance of a hydroperoxyl-like complex. The O-O bond is activated, leading to a weakened peroxo or superoxolike state, and consequently the reaction with CO to form CO_2 occurs with a small activation barrier of ~0.5 eV. A complete catalytic cycle of the water-enhanced CO oxidation is discussed.

DOI: 10.1103/PhysRevLett.95.106102 PACS numbers: 68.47.Jn, 68.43.Bc, 82.33.Hk

Unlike supported particles of larger sizes, or extended surfaces [1,2], small supported metal clusters were found to exhibit unique properties that originate from their highly reduced dimensions [3–6]. Recent joint experimental studies and theoretical investigations [6–8] using first-principles simulations on size-selected small gold clusters, Au_n ($20 \geq n \geq 2$), adsorbed on well characterized MgO(100) surfaces under ultra-high-vacuum conditions, revealed that gold octamers (Au_8) bound to oxygen vacancy F centers of the magnesia surface, are the smallest known gold heterogeneous catalysts that can oxidize CO into CO_2 at temperatures as low as 140 K. The same clusters adsorbed on a MgO defect-free surface are catalytically inactive for CO combustion [6–8]. In these investigations charging of the adsorbed metal cluster through partial electron transfer from the substrate F-center defect and subsequent occupation of the antibonding $2\pi^*$ orbital of O_2 occurs. This and the consequent activation of the O-O bond of the molecule adsorbed on the cluster (resulting in formation of peroxo or superoxo states), have been identified as underlying the catalytic activity.

Unlike other common catalysts [9], the presence of moisture is beneficial to gold catalysts [9–13], increasing their activity by up 2 orders of magnitude [9,12]. However, to date only a few experiments (focusing on high moisture levels) addressed the water enhancement mechanisms [9–13], and theoretical studies and/or microscopic understanding are lacking.

Here we investigate with the use of first-principles calculations the microscopic origins of the remarkable enhancement due to water of the catalytic activity of gold nanoclusters adsorbed on a *perfect* MgO(100) surface (or in the gas phase). We find that an adsorbed H_2O molecule serves as an "attractor" of O_2 to its vicinity, with the coadsorbed molecules forming a complex strongly bound to the gold cluster (even in the absence of defects, i.e., F centers, and consequent charging effects that, as mentioned above, play an important role under dry conditions). Formation of the complex involves partial sharing of a proton between the coadsorbed molecules, which in certain adsorption configurations is fully transferred to the O_2 molecule leading to a hydroperoxyl-like complex and a hydroxyl group. The calculations show that H_2O favors partial charging of the O_2 molecule through population of the antibonding molecular orbital, resulting in activation of the O-O bond, whose length extends to values characteristic of superoxo or peroxolike states. A reaction channel of the $O_2 \cdots H_2O$ complex (formed on the top facet of the supported gold octamer) with gaseous CO, occurring via an Eley-Rideal mechanism with an energy barrier of about 0.5 eV, is described, and a complete catalytic cycle is discussed. We also discuss briefly a Langmuir-Hinshelwood reaction path (with a similar barrier height), involving an H_2O molecule adsorbed on the MgO substrate near the supported cluster, with O_2, and CO molecules coadsorbed at the gold/MgO interface.

The quantum mechanical *ab initio* calculations [14] are based on spin-density functional theory with generalized gradient corrections (GGA) [15]. The wave functions are expanded in a plane-wave basis with a kinetic energy cutoff of 25 Ry. The core-valence interactions for Au, O, and H are described through the use of ultrasoft pseudopotentials [16] (with Au treated scalar relativistically [6–8]), and a norm-conserving pseudopotential is used for Mg [17]. The Brillouin zone of our simulation cell is sampled at the Γ point.

To focus on the influence of water on the chemical activity of gold in nanocatalytic reactions, we selected to treat here model systems that do not exhibit charging effects originating from excess electrons (as in free Au cluster anions [18–20]) or from defects at the metal-oxide surface [6–8]. Accordingly, we consider two free neutral Au clusters (Au_8 and Au_{30}), and in the case of a surface-supported cluster we model a gold octamer, Au_8, adsorbed on a defect-free MgO surface described by a two-layer MgO(100) $-$ (3×3) slab; properties of the perfect MgO(100) surface and the corresponding oxygen vacancy are well reproduced by a two-layer film [21].

O_2 *adsorption on free and supported gold clusters.*— While molecular oxygen does not adsorb on clean Au(110)

and (111) extended surfaces [22], it has been suggested that the adsorption propensity of O_2 to finite size Au particles is increased, particularly at low-coordinated sites [19,23,24]. For each of the relaxed configurations of O_2 at the various adsorption sites on the Au_8 and Au_{30} clusters, we obtain the adsorption energy, defined as the difference between the optimized energy of the combined system, $Au_n + O_2$, and that of the separated relaxed components, Au_n and O_2. Our calculations show that O_2 does not bind to Au_8 and for the larger cluster the adsorption energies at the various sites range only up to 0.4 eV (Table I).

Next we consider the properties of the gold octamer adsorbed on a defect-free MgO(100) surface. The presence of the support causes broadening of the O_2 adsorption energies distribution. Two spatial regions may be identified: (i) the top facet of the cluster, where O_2 adsorbs weakly (adsorption energies up to 0.1 eV), in agreement with other first-principles calculations [6,23,25], and (ii) peripheral sites (at the Au_8/MgO interface), where O_2 adsorbs with energies larger than 0.3 eV and up to 0.8 eV (Table I), with the O-O bond extended to 1.37–1.49 Å (i.e., in the range typical of superoxo, or peroxo states).

Coadsorption of O_2 *and* H_2O *on free and supported gold clusters.*—It has been established experimentally that extended clean gold surfaces are hydrophilic [26]. Our calculations show that water adsorbs (relatively weakly) on free and supported Au clusters (Table I), with adsorption energies that vary from 0.2 to 0.6 eV, and without apparent correlation between the adsorption strength and the coordination of the adsorption site. We also find that an adsorbed H_2O is an attractor for molecular O_2. Indeed, in the presence of an adsorbed water molecule O_2 preferentially adsorbs (in a singlet spin state) at a neighboring site (Fig. 1, top). Moreover, the coadsorbed O_2 does not show preference to particular sites on the gold cluster, and may take place even at sites where the adsorption of O_2 (without coadsorbed H_2O) is energetically unfavorable. In the case of free Au_8 and Au_{30} clusters our calculations give a range of coadsorption energies of 0.4–0.9 eV (Table I). These values are larger then the sum of the adsorption energies of the two separated species on the Au clusters, indicating that the coadsorption of H_2O and O_2 exhibit a synergetic effect, and implying possible formation of a stable complex of the two adsorbed molecules.

In the coadsorbed state on the free clusters the O_2 molecule shows peroxolike characteristics, with a bond length of about 1.45 Å (18% larger than the gas-phase value); comparison with the properties of O_2 adsorbed under dry conditions highlights the enhanced O-O bond activation induced by the H_2O molecule. In the coadsorbed configurations (see Fig. 1, top) the O-H bond of the H_2O molecule pointing toward the nearest oxygen atom of the O_2 elongates to 1.1 Å, with the distance between the two oxygens on the two sides of the proton being close to 2.5 Å (partial proton sharing). To estimate possible electronic charge rearrangement and charging effects in the coadsorbed system, we focus on the specific adsorption complex shown for Au_8 (see atomic configuration at the top left of Fig. 1). For this particular set of nuclear positions we calculate the difference between the electronic charge density of the full system and the sum of the densities of

TABLE I. Energies (in eV) for the adsorption and coadsorption of O_2 and H_2O on free (Au_8 and Au_{30}) clusters and on a gold octamer supported on MgO(100), i.e., Au_8/MgO. In the case of the Au_8/MgO system, results are given for both the adsorption on the top facet of the gold cluster (-T) and at the peripheral interface of the cluster with the substrate (-P).

	O_2	H_2O	O_2-H_2O
Au_8	Unbound	~0.3	0.4–0.9
Au_8	≤ 0.4	0.3–0.6	0.7–0.9
Au_8/MgO-T	≤ 0.1	0.2–0.3	0.5–1.2
Au_8/MgO-P	0.3–0.8	0.4–0.6	1.3–2.1

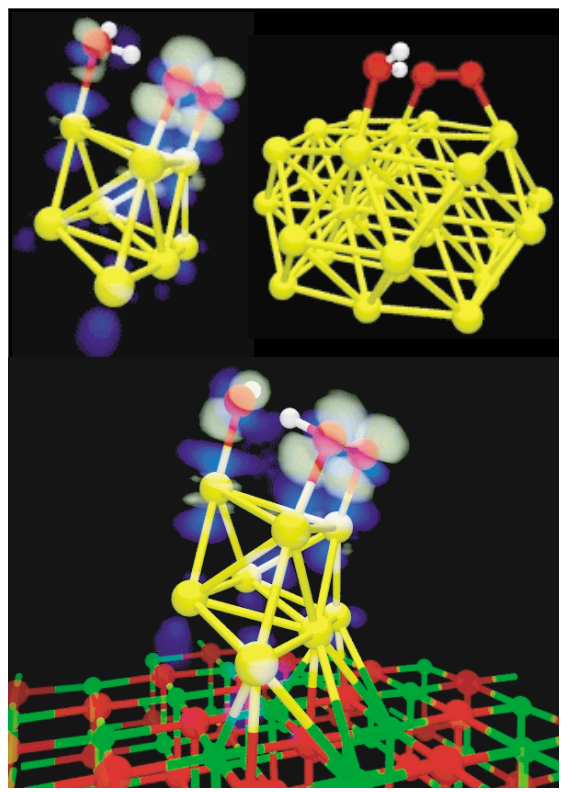

FIG. 1 (color). Relaxed atomic configurations of H_2O and O_2 coadsorbed on free Au_8 and Au_{30} clusters (top), and on Au_8/MgO(100) (bottom). For the free and supported Au_8 cases we display difference-charge density between the complete adsorption system and the separated Au_8/MgO(100) and $O_2 \cdots H_2O$ complex, superimposed on the atomic configuration. Charge depletion is shown in blue and charge accumulation in gray-white. Yellow, red, white, and green spheres correspond to Au, O, H, and Mg atoms, respectively.

the separated components (the Au_8 cluster and the $O_2 \cdots H_2O$ species, respectively, keeping the geometries as found for the adsorption system). This procedure allows us to assess the charge redistribution occurring by joining the Au cluster and the coadsorbed species. We find that electronic charge depleted in the region of the Au_8 cluster accumulates at the location of the adsorbed O_2 molecule (in particular in the originally empty $2\pi^*$ orbital, see gray-white lobes in Fig. 1, top left). Integrating over the semispaces defined by the normal plane bisecting the Au-O bonds yields an estimated charge transfer of about $0.27e$.

The optimized configurations of H_2O and O_2 coadsorbed on the top facet of Au_8/MgO are generally similar to those found for the unsupported clusters. However, in some occasions we observed that the proton (partially) shared by the H_2O and O_2 molecules may actually be considered as transferred to the O_2 species (see, e.g., bottom of Fig. 1). In such instances coadsorption leads to the formation of an OH and a hydroperoxyl-like (HO_2) group. The distance between the O atoms flanking the proton takes a value of about 2.49 Å, and for the H-O-O (hydroperoxyl) the H-O distance is 1.1 Å and the O-O bond length reaches a value of about 1.48 Å (that is 21% larger than in a free molecule), reflecting a very high degree of bond activation. The electronic charge density of the combined system, referenced to that of the separated Au_8/MgO and $OH \cdots HO_2$ components (Fig. 1, bottom), exhibits a charge redistribution pattern similar to that described above for the free Au cluster (Fig. 1, top left). In particular, charge analysis shows that an amount of approximately $0.31e$ is transferred from the Au_8/MgO system to the coadsorbed species; from similar analysis applied to the bare Au_8/MgO complex we estimate that upon adsorption an electronic charge of about $0.4e$ is transferred from the MgO substrate to the adsorbed Au_8 cluster.

These results suggest that the coadsorption of H_2O and O_2 stabilizes partially charged highly activated states of the adsorbed oxygen molecule (with the extra electronic charge donated by the underlying supported gold cluster). Such activated states include the hydroperoxyl-like intermediate shown at the bottom of Fig. 1, as well as a partially negatively charged oxygen molecule in a superoxo or peroxo state (with an O-O bond elongated by 0.1 to 0.2 Å, respectively, with reference to the free molecule), stabilized through a partial proton-sharing mechanism. No such bond activation is found for the adsorption of O_2 on the top facet of the supported gold octamer without water coadsorption (recall the small adsorption energies given for the Au_8-MgO-T configuration in Table I).

MgO surfaces are hydrophilic and H_2O molecules adsorb with energies of about 0.4 eV. In the vicinity of the peripheral interfacial sites of the Au cluster we find that the adsorption energy of H_2O increases by 0.1–0.2 eV (depending on the particular site and adsorption configuration); thus the gold cluster acts as an attractor for adsorbed water (reverse spillover). Hence, at the interface between the Au cluster and the MgO surface, peripheral sites show a high propensity to bind both H_2O and O_2 (Table I). The markedly larger binding energies of the coadsorbed complex (compared to the individual adsorbates) reflect a synergetic effect, expressed through the occurrence of the

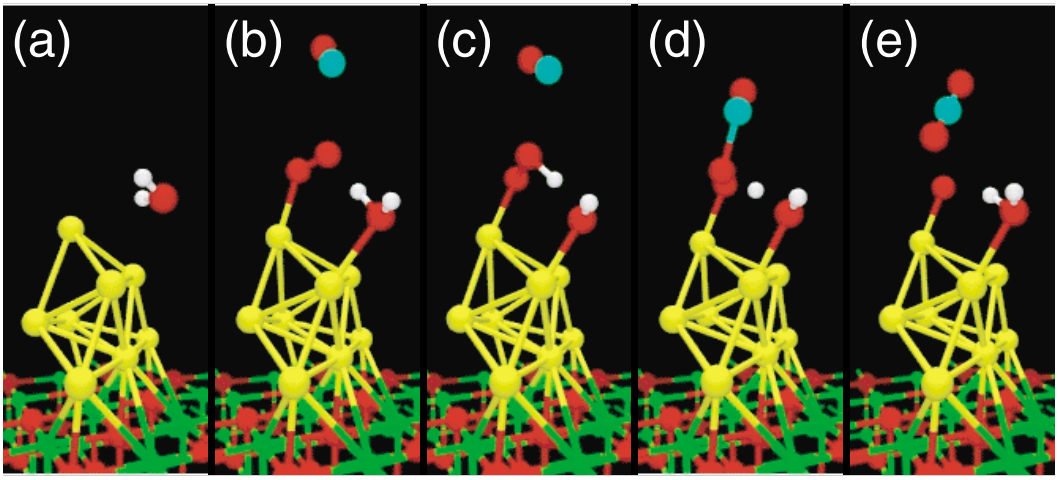

FIG. 2 (color). Relaxed atomic configurations displaying several stages in the simulation of the coadsorption of H_2O and O_2 on the top facet of a Au_8 cluster supported on MgO(100), and the subsequent reaction with gaseous CO to form CO_2. (a) The approach of an H_2O molecule to the cluster. (b) Coadsorbed H_2O (right) and O_2 (left) with an approaching CO. Note the preferential orientation of the H_2O and partial proton sharing. (c) CO induced proton transfer resulting in formation of a hydroperoxyl-like group (left) and a hydroxyl (right). (d) Transition-state configuration with the CO binding to the activated species. The proton is about midway between one of the oxygens of the transition-state complex (left) and the hydroxyl (right). (e) The proton shuttles back to reform an adsorbed H_2O, and the CO_2 product desorbs from the surface, leaving an adsorbed oxygen atom that reacts in the next step with a CO molecule to yield a second CO_2. Yellow, red, white, green, and aquamarine spheres correspond to Au, O, H, Mg, and C atoms, respectively.

aforementioned partial proton-sharing and proton-transfer processes.

To address the reactivity of O_2 coadsorbed with H_2O on the top facet of the adsorbed gold cluster we display in Fig. 2 a sequence of adsorption and reaction steps that result in the catalytic oxidation of CO. Starting from the bare Au_8/MgO system we adsorb first a H_2O molecule [Fig. 2(a)] and subsequently coadsorb an O_2 and expose the system to incident CO [see the proton-sharing configuration in Fig. 2(b)]. In Fig. 2(c) a proton-transfer process, induced by the incoming gaseous CO molecule, is shown, leading to formation of a hydroperoxyl-like complex. Upon reaction of the CO molecule with the complex the proton shuttles back toward the hydroxyl group [Fig. 2(d)], with the process culminating in the desorption of a CO_2 molecule and reformation of an adsorbed H_2O molecule that is preferentially oriented with respect to the remaining adsorbed oxygen atom, Fig. 2(e). The above Eley-Riedel-like reaction mechanism involves relatively low barriers, which we estimate from a constrained molecular dynamic approach [27]. We find that formation of the transition state [shown in Fig. 2(d)] entails a readily accessible energy barrier of $\sim$0.5 eV. An added CO molecule reacts readily (a barrier of 0.1 eV) with the single adsorbed oxygen atom, and the (barrierless) desorption of the CO_2 product closes the catalytic cycle.

In the above we focused on reactions occurring on the top facet of the Au_8 cluster, since in this case the enhancement effect of the H_2O is illustrated most dramatically (i.e., without the coadsorbed H_2O, binding of O_2 to the cluster is exceedingly weak, see Table I). Nevertheless, for completeness we note that a peripherally adsorbed O_2 reacts with a CO molecule adsorbed in its vicinity with a Langmuir-Hinshelwood reaction barrier of 0.4 eV (with or without a neighboring coadsorbed H_2O molecule). The barrier for desorption of the CO_2 product which is 0.6 eV under dry conditions is lowered to 0.3 eV with coadsorbed H_2O.

In summary, our first-principles investigations revealed a significant enhancement of the binding and activation of O_2, occurring upon coadsorption of O_2 and water on small Au clusters supported on defect-free MgO(100), as well as on gas-phase neutral clusters. Underlying the water-induced increased catalytic activity of gold nanoclusters toward oxidation of CO, is the formation of a complex between the adsorbed molecules involving partial proton sharing, or proton transfer resulting in the appearance of a hydroperoxyl-like intermediate. The activated (weakened) O-O bond in the complex shows superoxo or peroxolike characteristics (e.g., increase in the bond length by 0.1–0.2 Å compared to the gas-phase value), and consequently the reaction with CO may occur readily with a relatively low barrier of 0.5 eV (either through an Eley-Rideal or Langmuir-Hinshelwood mechanism, depending on the adsorption site). A complete catalytic cycle of the water-enhanced CO oxidation was discussed. We trust that these findings would provide the impetus for future theoretical and experimental investigations of the effect of water on nanocatalytic processes.

We acknowledge support from the AFOSR and DOE. Computations were performed at the DOE National Energy Research Scientific Computing Center (NERSC), and the DOD computers, via the High Performance Computing Program.

[1] C. R. Henry, Surf. Sci. Rep. **31**, 231 (1998).
[2] G. Ertl and H.-J. Freund, Phys. Today **52**, No. 1, 32 (1999).
[3] M. Haruta, Catal Today **36**, 153 (1997).
[4] G. C. Bond and D. T. Thompson, Catal. Rev. Sci. Eng. **41**, 319 (1999).
[5] M. Valden, X. Lai, and D. W. Goodman, Science **281**, 1647 (1998).
[6] A. Sanchez *et al.*, J. Phys. Chem. A **103**, 9573 (1999).
[7] H. Häkkinen *et al.*, Angew. Chem., Int. Ed. **42**, 1297 (2003).
[8] B. Yoon *et al.*, Science **307**, 403 (2005).
[9] M. Haruta, in *Catalytic Science and Technology*, edited by S. Yoshida, N. Takezawa, and T. Ono *et al.*, (Kodansha, Tokyo, 1991), Vol. 1, p. 331.
[10] M. Daté and M. Haruta, J. Catal. **201**, 221 (2001).
[11] M. Daté *et al.*, Catal Today **72**, 89 (2002).
[12] M. Daté *et al.*, Angew. Chem., Int. Ed. **43**, 2129 (2004).
[13] H. H. Kung *et al.*, J. Catal. **216**, 425 (2003).
[14] A. Pasquarello *et al.*, Phys. Rev. Lett. **69**, 1982 (1992); K. Laasonen *et al.*, Phys. Rev. B **47**, 10 142 (1993).
[15] J. P. Perdew, K. Burke, and M. Ernzerhof, Phys. Rev. Lett. **77**, 3865 (1996). The accuracy of the DFT/GGA calculations was checked for judiciously selected small systems; e.g., for the ground state of the $(H_2O)_2$ cluster we find a binding energy of 0.28 eV compared to a measured value of 0.24 eV, and the calculated geometry is close to the experimental one.
[16] D. Vanderbilt, Phys. Rev. B **41**, 7892 (1990).
[17] N. Troullier and J. L. Martins, Phys. Rev. B **43**, 1993 (1991).
[18] H. Häkkinen and U. Landman, J. Am. Chem. Soc. **123**, 9704 (2001).
[19] B. Yoon *et al.*, J. Phys. Chem. A **107**, 4066 (2003).
[20] L. D. Socaciu *et al.*, J. Am. Chem. Soc. **125**, 10 437 (2003).
[21] L. Giordano *et al.*, Phys. Rev. B **67**, 045410 (2003).
[22] J. J. Pireaux *et al.*, Surf. Sci. **141**, 211 (1984); Y. Xu and M. Mavrikakis, J. Phys. Chem. B **107**, 9290 (2003).
[23] N. Lopez and J. K. Nørskov, J. Am. Chem. Soc. **124**, 11 262 (2002).
[24] G. Mills *et al.*, Chem. Phys. Lett. **359**, 493 (2002).
[25] L. M. Molina and B. Hammer, Phys. Rev. B **69**, 155424 (2004).
[26] T. Smith, J. Colloid Interface Sci. **75**, 51 (1980).
[27] A. Bongiorno and A. Pasquarello, Phys. Rev. Lett. **93**, 86 102 (2004).